Mercury

International Edition: DOI: 10.1002/anie.201606015
German Edition: DOI: 10.1002/ange.201606015

Selective and Efficient Removal of Mercury from Aqueous Media with the Highly Flexible Arms of a BioMOF

Marta Mon, Francesc Lloret, Jesús Ferrando-Soria, Carlos Martí-Gastaldo, Donatella Armentano,* and Emilio Pardo**

Abstract: *A robust and water-stable metal–organic framework (MOF), featuring hexagonal channels decorated with methionine residues (**1**), selectively captures toxic species such as CH_3Hg^+ and Hg^{2+} from water. **1** exhibits the largest Hg^{2+} uptake capacity ever reported for a MOF, decreasing the $[Hg^{2+}]$ and $[CH_3Hg^+]$ concentrations in potable water from highly hazardous 10 ppm to the much safer values of 6 and 27 ppb, respectively. Just like with biological systems, the high-performance metal capture also involves a molecular recognition process. Both CH_3Hg^+ and Hg^{2+} are efficiently immobilized by specific conformations adopted by the flexible thioether "claws" decorating the pores of **1**. This leads to very stable structural conformations reminiscent of those responsible for the biological activity of the enzyme mercury reductase (MR).*

Even though the WHO is strongly trying to raise awareness for reducing the amount of mercury in domestic tools and in different industrial sectors (e.g., chloralkali plants and vinyl chloride monomer production),[1] the world's annual mercury consumption was still estimated to be up to 2000 tons in 2016.[2] Environmental contamination by the interconvertible[3,4] Hg^{2+} and CH_3Hg^+ cations is of great concern from the viewpoint of human health.[5] In this sense, the very easy air and water transportation of both species, as well as their long atmospheric lifetimes, make them very widespread environment pollutants.[6] As a consequence, high concentrations of mercury can be found not only in fish,[7] but also in agricultural crops[8] and in animals living in non-marine habitats.[9] On this basis, the search for sustainable green methods for the effective capture and removal of the different chemical forms of mercury is mandatory and has attracted a great deal of interest.[10–15]

[*] M. Mon, Prof. Dr. F. Lloret, Dr. J. Ferrando-Soria, Dr. C. Martí-Gastaldo, Dr. E. Pardo
Instituto de Ciencia Molecular (ICMOL)
Universitat de València
Paterna 46980, València (Spain)
E-mail: jesus.ferrando@uv.es
emilio.pardo@uv.es
Dr. D. Armentano
Dipartimento di Chimica e Tecnologie Chimiche (CTC)
Università della Calabria
87030, Rende, Cosenza (Italy)
E-mail: donatella.armentano@unical.it

Supporting information and the ORCID identification number(s) for the author(s) of this article can be found under http://dx.doi.org/10.1002/anie.201606015.

Metal–organic frameworks (MOFs)[16–20] have already been shown to perform very well in the selective capture and/or separation of gases,[21] metals,[22] and small molecules.[23] Most of these thrilling properties of MOFs, which are related to their porous character and rich host–guest chemistry,[24] can be tuned by an appropriate functionalization of the channels. Taking advantage of the methods provided by coordination chemistry, an accurate design effort[25] should thus lead to water-stable[26,27] MOFs for use as "mercury receptors".[28–33]

Nature has evolved mechanisms to effectively distinguish one metal from another. How metal ions move to and from their target destinations in the active site of a metalloenzyme, or as structural components of other biomolecules such as nucleic acids, efficiently contributes to the regulation of biological processes. An interesting example within this context is the mercury reductase (MR),[34] a redox enzyme that catalyzes the reduction of highly toxic Hg^{2+} into more benign Hg^0. The active center of this enzyme represents a source of inspiration for coordination chemists working in the area of mercury detoxification, and efforts trying to mimic it have been pursued.[34] MOFs could thus also find application as vessels encapsulating biological systems.[35]

Among the large class of MOFs, bioMOFs,[36] designed from naturally occurring organic ligands, are highly promising for both mercury removal and biomimicry. In this context, we have recently reported a robust and water-stable, heterobimetallic calcium(II)/copper(II) three-dimensional (3D) bioMOF,[37] which was synthesized by using the enantiopure bis[(*S*)-methionine]oxalyl diamide[37–40] ligand derived from the natural amino acid L-methionine (see the Supporting Information, Scheme S1). This porous material with the formula $\{Ca^{II}Cu^{II}_6[(S,S)\text{-methox}]_3(OH)_2(H_2O)\}\cdot 16H_2O$ (**1**) features functional channels decorated with thioalkyl chains, which account for its strong and selective affinity for different gold salts as well as excellent catalytic activity.[37] On the basis of the well-known affinity of mercury for sulfur atoms, we have further extended this work to evaluate the efficiency of **1** in the capture and removal of Hg^{2+} and CH_3Hg^+ from aqueous media (Scheme S2). The high selectivity and capture capacity of **1** towards these hazardous species from aqueous solutions render it a good mercury removal agent, expanding the concept of "metal receptors" from biology to nanotechnology applications.

We began our study by investigating the efficiency of **1** in the capture of $HgCl_2$ and CH_3HgCl salts from water. However, its maximum loading capacity was determined from water and water/methanol, respectively. Thus crystals of **1** were soaked in saturated solutions of $HgCl_2$ (H_2O) and

CH_3HgCl (H_2O/MeOH 1:1) for 72 h. The final contents and the kinetic profiles of both adsorption processes were determined through ICP-MS and SEM/EDX analyses by measuring the increase in the concentration of the corresponding mercury salts within the MOF at specific time intervals (Figure S1 and Table S1).

Overall, **1** exhibited high and moderate affinities for $HgCl_2$ and CH_3HgCl in water and water/methanol solutions, respectively, through single-crystal to single-crystal (SC to SC) processes[38–40] (see the Supporting Information). The $HgCl_2$ adsorption proceeded by a two-step process that involved a first, extremely fast adsorption of three molecules of $HgCl_2$ per formula unit and a second, slower adsorption process to reach a final loading of up to five molecules (Figure S1). Owing to these particular kinetics, two different adsorbates were obtained with $HgCl_2$. In turn, the CH_3HgCl adsorption was found to be slower than that of $HgCl_2$, reaching a final loading of only one molecule of CH_3HgCl per formula unit (Figure S1). The lower loading and adsorption rate of CH_3HgCl can be explained in terms of its poorer solubility and/or its weaker affinity for thioether groups but also in terms of structural considerations (see below).[41] Therefore, three adsorbates with the formulas $(HgCl_2)_3\{Ca^{II}Cu^{II}_6[(S,S)\text{-methox}]_3(OH)_2(H_2O)\}\cdot 8H_2O$ ($3HgCl_2$@**1**), $(HgCl_2)_5\{Ca^{II}Cu^{II}_6[(S,S)\text{-methox}]_3(OH)_2(H_2O)\}\cdot 4H_2O$ ($5HgCl_2$@**1**), and $(CH_3HgCl)\{Ca^{II}Cu^{II}_6[(S,S)\text{-methox}]_3(O)(CH_3OH)_2\}\cdot 5H_2O$ (CH_3HgCl@**1**) were obtained and characterized by ICP analyses (see the Experimental Section in the Supporting Information).

These results confirmed that **1** is capable of purifying contaminated water solutions. In particular, they indicate maximum recoveries of 900 ($HgCl_2$) and 166 mg (CH_3HgCl) per g of **1** in $5HgCl_2$@**1** and CH_3HgCl@**1**, respectively. Such a high loading of $HgCl_2$ in water is close enough to the maximum loading ever observed in a porous material (1 g g^{-1} MOF)[11] and constitutes a benchmark value for MOFs. Even if rather low compared to $HgCl_2$ adsorption, the CH_3HgCl uptake from water/methanol confirmed the suitability of this porous material for the capture of this mercury species. Remarkably, this is, to the best of our knowledge, the very first time that a MOF was used to capture CH_3Hg^+. Moreover, the $HgCl_2$ and CH_3HgCl adsorption processes were found to be fully reversible, as the mercury salts were easily extracted with dimethyl sulfide (see the Experimental Section in the Supporting Information), so that **1** can be reused as often as needed; this was confirmed by chemical analysis (**1′**; see the Supporting Information), the PXRD pattern of the material after the extraction process (Figure S2), and a second adsorption process carried out with the reused material (Table S4).

The structure of **1** consisted of a chiral honeycomb-like 3D calcium(II)/copper(II) network featuring functional hexagonal channels of approximately 0.3 nm where the highly flexible ethylenethiomethyl chains of the methionine amino acid remained confined (Figures 1b and 2a). This uninodal sixfold-connected net (Schläfli symbol 4^96^6), is built from *trans*-oxamidato-bridged dicopper(II) units, $\{Cu^{II}_2[(S,S)\text{-methox}]\}$ (Figure 1a), which act as linkers between the Ca^{II} ions through the carboxylate groups (Figure 1c). Neighboring

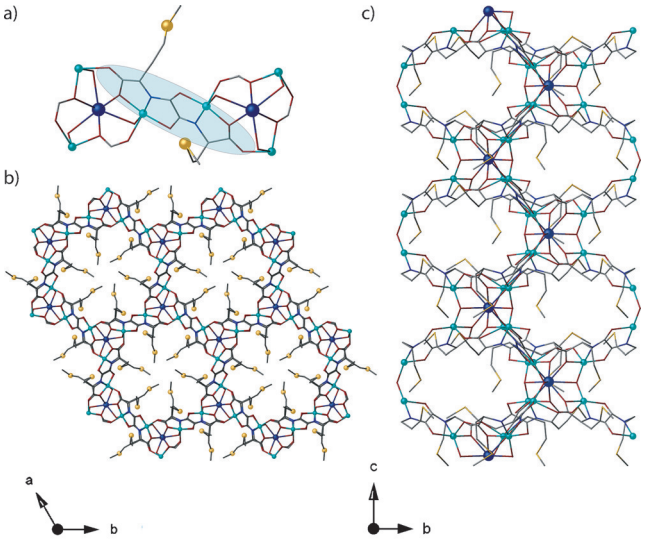

Figure 1. a) Fragment of **1** showing the dianionic bis(hydroxo) dicopper(II) building blocks. Views of a fragment of **1** in the *ab* (b) and *bc* (c) planes, respectively. Cu, Ca, and S atoms are represented by green, purple, and yellow spheres, respectively, whereas the ligands (except sulfur) are depicted as sticks (C gray, O red, N blue).

Cu^{2+} and Cu^{2+}/Ca^{2+} ions are further interconnected by aqua/hydroxo groups (in a 1:2 statistical distribution) linked in a μ_3 fashion (Figure 1c).

The crystal structures of all three adsorbates, $3HgCl_2$@**1**, $5HgCl_2$@**1**, and CH_3HgCl@**1**, could be resolved by single-crystal X-ray diffraction, giving unprecedented insight into the S···Hg interaction as well as the molecular recognition process involved in the mercury capture. Indeed, this is the very first time that the real structures of such adsorbates have been experimentally determined, allowing us to confirm and even to rigorously visualize the accomplished capture and the exceptional structural adaptability of the system. They all crystallized in the chiral $P6_3$ space group of the hexagonal system (Table S2) like precursor **1** (Figures 1, 2, and S3–S7).[37] The crystal structures of the three adsorbates clearly confirmed the presence of $HgCl_2$ and CH_3HgCl guest molecules hosted in the hexagonal nanopores of **1**;[42] they are recognized by the thioether arms of the methionine residues and confined into the channels through S···Hg interactions. Yet, they showed different arrangements depending on the degree of loading or the nature of the guest molecule, leading to either discrete mono- ($3HgCl_2$@**1** and CH_3HgCl@**1**) or dinuclear species ($5HgCl_2$@**1**; Figures 2 and S7). This striking feature of **1** is likely related to the intrinsic flexibility and structural adaptability[43–47] of its functional channels (Figure S6), which must be at the origin of the tunable structure/conformation of the thioether chains that are reminiscent of the MR enzyme (Scheme S3).[34]

The Hg^{2+} ions from both the mononuclear $HgCl_2$ and CH_3HgCl fragments in $3HgCl_2$@**1** and CH_3HgCl@**1** (Figure 2a and c, respectively) and the chloride-bridged dinuclear $[Hg_2(\mu\text{-}Cl)_2Cl_2]$ entities in $5HgCl_2$@**1** (Figure 2b) are tetracoordinated, being further grasped by two sulfur atoms from the thioether groups belonging to the amino acid residues of

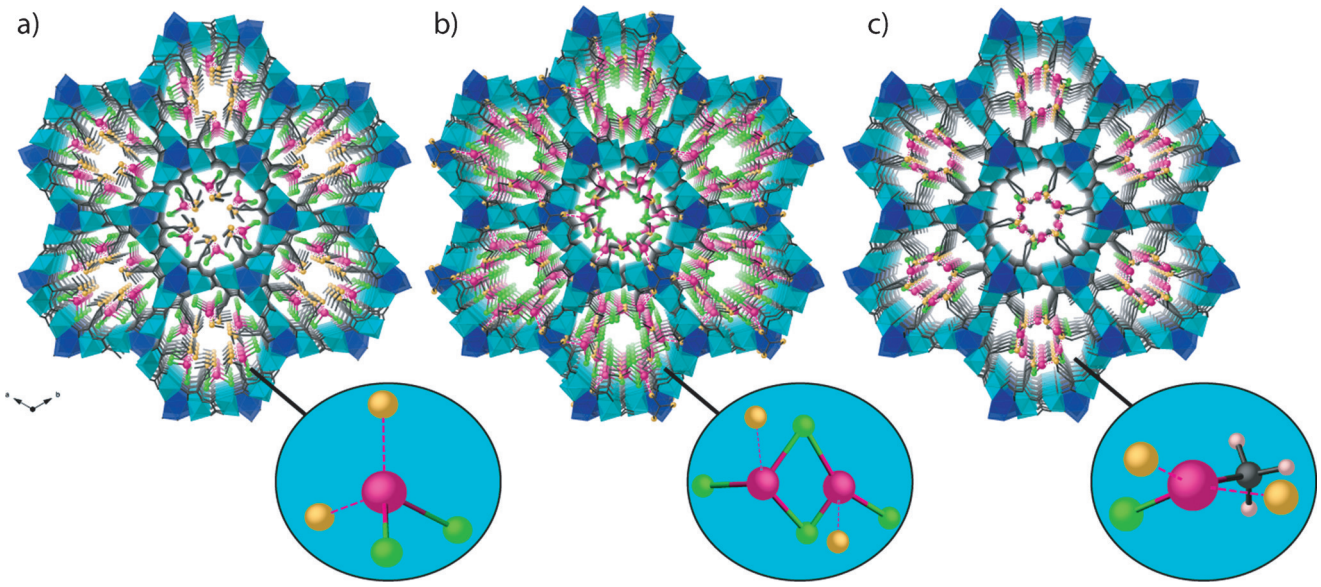

Figure 2. Perspective views along the crystallographic *c* axis of the porous structures of 3 $HgCl_2$@**1** (a), 5 HgCl2@**1** (b), and CH_3HgCl@**1** (c). Cu and Ca atoms are represented by cyan and blue polyhedra, respectively. Hg and Cl atoms are depicted as purple and green spheres, whereas sulfur and carbon atoms from the methionine residues and the methyl groups, respectively, are shown as yellow and gray spheres. The remaining carbon, nitrogen, and oxygen atoms from the ligand are shown as sticks. Free water solvent molecules omitted for clarity. The blue insets highlight the coordination environment of the captured mercury species.

methionine-disubstituted oxamidato ligands (Figures S3–S5). They exhibit a somewhat distorted (3 $HgCl_2$@**1** and 5 $HgCl_2$@**1**) or highly distorted (CH_3HgCl@**1**) tetrahedral geometry, most likely because of the steric constraints imposed by the network (Figures 2 and S3–S5). The Hg–S bond lengths [2.29(3) and 2.60(3) Å (3 $HgCl_2$@**1**), 2.49(3) and 2.96(3) Å (5 $HgCl_2$@**1**), and 2.78(7) and 2.85(7) Å (CH_3HgCl@**1**)] are in the range of those found in the literature.[48–50] Furthermore, the rather short value of the intradimer Hg···Hg separation in 5 $HgCl_2$@**1** [2.89(2) Å; Figures 2b and S4] indicates the presence of a metal–metal bond.[51]

In 3 $HgCl_2$@**1,** both thioether "arms" show a distended conformation and target a $HgCl_2$ molecule with high affinity, adopting a stable conformation (Figures 2a, S3a, and S5a) evocative of that found in the MR binding site,[34] where the sulfur atoms are those of thiolate groups of cysteine residues in the protein backbone while additional oxygen atoms from tyrosine residues take the place of the chlorine ones. Similarly, the two distended thioether arms in CH_3HgCl@**1** target a CH_3HgCl molecule each, but in a different conformation (Figure S6c), which is likely driven by host–guest methyl–methyl repulsive interactions between the Hg–CH_3 units and the S–CH_3 groups from methionine (Figures 2c, S3c, and S5b), giving rise to a very close-packed structure with no more empty space, which plausibly accounts for the lower loading (Figure S7f). In contrast, only one of the two thioether arms adopts a distended conformation in 5 $HgCl_2$@**1** (Figures 2b, S3b, and S4). Most likely, the steric hindrance resulting from the higher number of molecules packed in such a confined space caused their aggregation into less hindered dimers and, at the same time, forced the flexible ethylenethiomethyl chains to adopt a highly bent conformation with their methyl groups pointing out of the pores (Figures S6 and S7).

The experimental powder X-ray diffraction (PXRD) patterns of polycrystalline samples of 3 $HgCl_2$@**1**, 5 $HgCl_2$@**1**, and CH_3HgCl@**1** are consistent with the calculated ones (Figures 3 and S8), confirming the purity and homogeneity of the bulk samples. The dramatic changes in the relative intensities of their peaks compared to their precursor **1** (Figure S8) is particularly relevant. While the lower-angle peaks decrease in intensity, the higher-angle peaks become

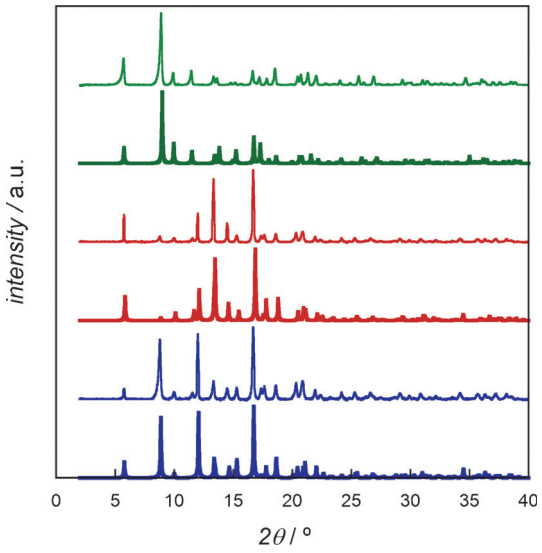

Figure 3. Calculated (bold lines) and experimental (solid lines) PXRD pattern profiles of 3 $HgCl_2$@**1** (blue), 5 $HgCl_2$@**1** (red), and CH_3HgCl@**1** (green) in the 2θ range 2.0–40.0°.

more intense. This behavior, which is accentuated in $3\,HgCl_2$@**1** and $5\,HgCl_2$@**1** owing to their higher loading, is clearly indicative of a significant increase in the electron densities in the channels filled with the heavy metals.[28] The water contents were estimated by thermogravimetric analysis (TGA, Figure S9).

Finally, experiments evaluating the selectivity of **1** towards $HgCl_2$ and CH_3HgCl and its efficiency in cleaning contaminated water as well as the kinetic profiles of these processes were designed and carried out in duplicate. First, a polycrystalline sample of **1** (50 mg) was soaked in 10 ppm aqueous and H_2O/CH_3OH solutions of $HgCl_2$ and CH_3HgCl, respectively, containing also 10 ppm of other ions usually present in water, such as Na^+, K^+, Ca^{2+}, Mg^{2+}, HCO_3^-, Cl^-, and NO_3^-, for one week at neutral pH. ICP-MS analyses every 24 h indicated that only the mercury salts were adsorbed by **1**.[52] Second, the kinetic profile of each mercury removal process was established. With that purpose and aiming at assessing the process applicability of this material, polycrystalline samples of **1** were mixed with the commercial polymer Matrimid in a ratio of 80:20 to give extruded pellets[53] of about 1–3 mm in diameter (see the Supporting Information), which allow for easier handling and long-term stability (Figure 4). PXRD measurements confirmed that this composite was isostructural with **1** (Figure S8c). Then, 60 mg of these pellets were soaked in 10 mL of aqueous solutions of $HgCl_2$ or CH_3HgCl (10 ppm) at neutral pH.

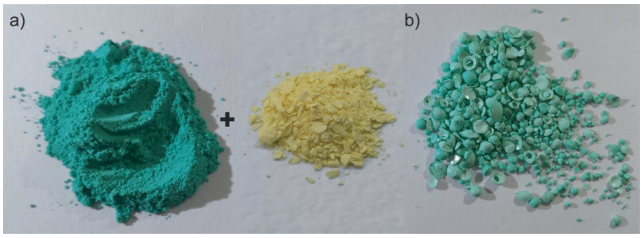

Figure 4. Photographs of powdered polycrystalline samples of **1** (left), Matrimid (middle), and the resulting extruded pellets (right).

The kinetics of the adsorption process, as well as the efficiency of the mercury removal, were determined by ICP-MS and SEM/EDX analysis by measuring the decrease in the concentration of each mercury salt after immersion of the pellets in the corresponding aqueous solution (Figure 5 and Table S3) at specific time intervals (0–10080 min). Overall, the experimental results showed that **1** adsorbs both mercury salts in a very fast, selective, and reversible manner. Remarkably, the $HgCl_2$ and CH_3Hg^+ concentrations in water were reduced from dangerous 10 ppm to extremely low levels of about 5 and 27 ppb after capturing 99.95 % and 99.0 % of the dissolved $HgCl_2$ and CH_3HgCl salts, respectively, which is within the permissible limits for Hg^{2+} ions in potable water.[1]

This high mercury-capture performance is comparable to that exhibited by the most efficient previously reported thiol-functionalized porous systems.[11,29,54,55] This fact is particularly striking considering the strong affinity of mercury for thiol groups compared to softer thioether moieties,[29] such as

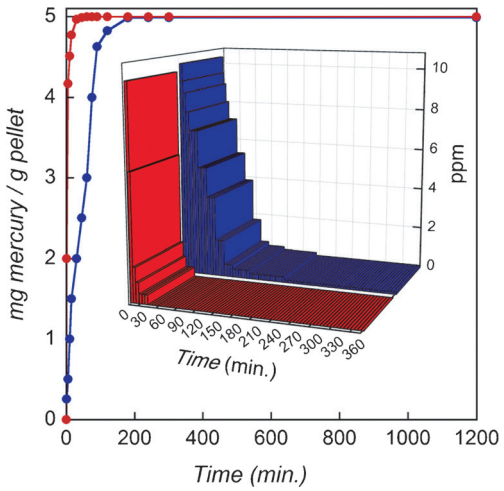

Figure 5. Hg^{2+} (red) and CH_3Hg^+ (blue) adsorption with time (first 1200 min) after soaking pellets of **1** in 10 ppm aqueous solutions of each species. The inset shows the decrease in $[Hg^{2+}]$ (red) and $[CH_3Hg^+]$ (blue) within the corresponding solutions.

those decorating the channels of **1**. This particularly good performance of a thioether-based system can be understood with the help of the X-ray crystallographic data. For instance, $HgCl_2$ is perfectly blocked and anchored within the channels of the heterobimetallic 3D network with the help of the sulfur atoms of two thioether groups, yielding a steady pseudo-tetrahedral geometry, which is allowed by the extreme flexibility of this system. In fact, the structures of the three different adsorbates of **1** clearly show that such a bioMOF is prone to discriminate metals as metalloproteins do in biological systems. In this sense, the high similarity between the coordination environment of Hg^{2+} in $3\,HgCl_2$@**1** and the binding site of MR most likely accounts for its high selectivity and chemical stability. Furthermore, the structure of $5\,HgCl_2$@**1** confirmed that for a higher loading of $HgCl_2$ to be reached, a dimerization reaction involving $HgCl_2$ molecules must occur. Thus **1** constitutes a good metal receptor for mercury salts, imitating the MR, which holds the metal ion in such a way that it can be readily transferred to an appropriate acceptor, such as sulfur-containing solvents in our case. Such intermolecular transfer processes are well-known in biology, and **1** further demonstrates that such processes can also occur through specific MOF complexes that are quickly formed and mediate intermolecular metal–ligand exchange as it happens in nature.

In summary, we have reported the selective capture of the most harmful forms of mercury from water with an inexpensive and environmentally friendly bioMOF (**1**) that can be easily prepared in large amounts. Resolution of the crystal structures of the mercury-containing adsorbates $3\,HgCl_2$@**1**, $5\,HgCl_2$@**1**, and CH_3HgCl@**1** gave unprecedented snapshots of the interaction between the mercury ions and the sulfur atoms from the thioether chains decorating the channels of the MOF. Indeed, they show the very high flexibility of these thioether arms in the selective mercury capture in a similar manner to that seen in biological systems and protein receptors. This flexibility accounts for the selectivity and

efficiency of the capture process. As a result of the adaptability of these amino acid residues to accommodate each harmful mercury species, this porous material is the first MOF that is capable of capturing highly toxic CH_3Hg^+ from water. Moreover, **1** exhibits the highest $HgCl_2$ loading capability ever reported for a MOF and is capable of cleaning contaminated water to permissible limits.

Acknowledgements

This work was supported by MINECO (Spain; Projects CTQ2013-46362-P, CTQ2013-44844-P, and Excellence Unit "Maria de Maeztu" MDM-2015-0538) and the Ministero dell'Istruzione, dell'Università e della Ricerca (Italy). M.M. thanks MINECO and the Universitat de València for predoctoral contracts. We also thank the Ramón y Cajal Program and the "Convocatoria 2015 de Ayudas Fundación BBVA a Investigadores y Creadores Culturales" (E.P. and J.F.-S.).

Keywords: bioMOFs · environmental chemistry · mercury · mercury reductase · metal–organic frameworks

How to cite: *Angew. Chem. Int. Ed.* **2016**, *55*, 11167–11172
Angew. Chem. **2016**, *128*, 11333–11338

[1] World Health Organisation, Guidelines for Drinking-Water Quality, Fourth Edition, **2011**.
[2] "https://mcgroup.co.uk/researches/mercury".
[3] X. Lu et al., *Environ. Sci. Technol.* **2016**, *50*, 4366–4373.
[4] Z. Ci, X. Zhang, Y. Yin, J. Chen, S. Wang, *Environ. Sci. Technol.* **2016**, *50*, 2371–2380.
[5] M. Horvat, *Trace Element Speciation for Environment, Food and Health*, Royal Society of Chemistry, Cambridge, **2001**.
[6] F. De Simone, C. N. Gencarelli, I. M. Hedgecock, N. Pirrone, *Environ. Sci. Technol.* **2016**, *50*, 5154–5162.
[7] M. Sadiq, *Toxic Metal Chemistry in Marine Environments*, Marcel Dekker, New York, **1992**.
[8] Y. Lin, Y. Yang, Y. Li, L. Yang, X. Hou, X. Feng, C. Zheng, *Environ. Sci. Technol.* **2016**, *50*, 2468–2476.
[9] T. W. Clarkson, *Trace Elements in Human and Animal Nutrition*, Elsevier, Heidelberg, **1987**, pp. 417–428.
[10] N. Dave, M. Y. Chan, P.-J. J. Huang, B. D. Smith, J. Liu, *J. Am. Chem. Soc.* **2010**, *132*, 12668–12673.
[11] B. Li, Y. Zhang, D. Ma, Z. Shi, S. Ma, *Nat. Commun.* **2014**, *5*, 5537.
[12] M. Banerjee, R. Karri, K. S. Rawat, K. Muthuvel, B. Pathak, G. Roy, *Angew. Chem. Int. Ed.* **2015**, *54*, 9323–9327; *Angew. Chem.* **2015**, *127*, 9455–9459.
[13] S.-Y. Ding, M. Dong, Y.-W. Wang, Y.-T. Chen, H.-Z. Wang, C.-Y. Su, W. Wang, *J. Am. Chem. Soc.* **2016**, *138*, 3031–3037.
[14] Y. Oh, C. D. Morris, M. G. Kanatzidis, *J. Am. Chem. Soc.* **2012**, *134*, 14604–14608.
[15] K. S. Subrahmanyam, C. D. Malliakas, D. Sarma, G. S. Armatas, J. Wu, M. G. Kanatzidis, *J. Am. Chem. Soc.* **2015**, *137*, 13943–13948.
[16] G. Férey, *Chem. Soc. Rev.* **2008**, *37*, 191–214.
[17] J. R. Long, O. M. Yaghi, *Chem. Soc. Rev.* **2009**, *38*, 1213–1214.
[18] H. Furukawa, K. E. Cordova, M. O'Keeffe, O. M. Yaghi, *Science* **2013**, *341*, 974.
[19] M. Eddaoudi, D. F. Sava, J. F. Eubank, K. Adil, V. Guillerm, *Chem. Soc. Rev.* **2015**, *44*, 228–249.
[20] Y. Cui, B. Li, H. He, W. Zhou, B. Chen, G. Qian, *Acc. Chem. Res.* **2016**, *49*, 483–493.
[21] J. Li, J. Sculley, H. Zhou, *Chem. Rev.* **2012**, *112*, 869–932.
[22] S. Yuan, Y.-P. Chen, J. Qin, W. Lu, X. Wang, Q. Zhang, M. Bosch, T.-F. Liu, X. Lian, H.-C. Zhou, *Angew. Chem. Int. Ed.* **2015**, *54*, 14696–14700; *Angew. Chem.* **2015**, *127*, 14909–14913.
[23] J. Ferrando-Soria et al., *J. Am. Chem. Soc.* **2012**, *134*, 15301–15304.
[24] Y. Inokuma, T. Arai, M. Fujita, *Nat. Chem.* **2010**, *2*, 780–783.
[25] S. Kitagawa, R. Matsuda, *Coord. Chem. Rev.* **2007**, *251*, 2490–2509.
[26] Q. Yang et al., *Angew. Chem. Int. Ed.* **2013**, *52*, 10316–10320; *Angew. Chem.* **2013**, *125*, 10506–10510.
[27] N. T. T. Nguyen, H. Furukawa, F. Gándara, H. T. Nguyen, K. E. Cordova, O. M. Yaghi, *Angew. Chem. Int. Ed.* **2014**, *53*, 10645–10648; *Angew. Chem.* **2014**, *126*, 10821–10824.
[28] J. He, K.-K. Yee, Z. Xu, M. Zeller, A. D. Hunter, S. S.-Y. Chui, C.-M. Che, *Chem. Mater.* **2011**, *23*, 2940–2947.
[29] K.-K. Yee, N. Reimer, J. Liu, S.-Y. Cheng, S.-M. Yiu, J. Weber, N. Stock, Z. Xu, *J. Am. Chem. Soc.* **2013**, *135*, 7795–7798.
[30] T. Liu, J.-X. Che, Y.-Z. Hu, X.-W. Dong, X.-Y. Liu, C.-M. Che, *Chem. Eur. J.* **2014**, *20*, 14090–14095.
[31] F. Luo, J. L. Chen, L. L. Dang, W. N. Zhou, H. L. Lin, J. Q. Li, S. J. Liu, M. B. Luo, *J. Mater. Chem. A* **2015**, *3*, 9616–9620.
[32] K.-K. Yee, Y.-L. Wong, M. Zha, R. Y. Adhikari, M. T. Tuominen, J. He, Z. Xu, *Chem. Commun.* **2015**, *51*, 10941–10944.
[33] A. Chakraborty, S. Bhattacharyya, A. Hazra, A. C. Ghosh, T. K. Maji, *Chem. Commun.* **2016**, *52*, 2831–2834.
[34] P. Lian et al., *Biochemistry* **2014**, *53*, 7211–7222.
[35] P. Li, J. A. Modica, A. J. Howarth, E. L. Vargas, P. Z. Moghadam, R. Q. Snurr, M. Mrksich, J. T. Hupp, O. K. Farha, *ChemistrySelect* **2016**, *1*, 154–169.
[36] A. C. McKinlay, R. E. Morris, P. Horcajada, G. Férey, R. Gref, P. Couvreur, C. Serre, *Angew. Chem. Int. Ed.* **2010**, *49*, 6260–6266; *Angew. Chem.* **2010**, *122*, 6400–6406.
[37] M. Mon, J. Ferrando-Soria, T. Grancha, F. R. Fortea-Pérez, J. Gascon, A. Leyva-Pérez, D. Armentano, E. Pardo, *J. Am. Chem. Soc.* **2016**, *138*, 7864–7867.
[38] T. Grancha, J. Ferrando-Soria, H.-C. Zhou, J. Gascon, B. Seoane, J. Pasán, O. Fabelo, M. Julve, E. Pardo, *Angew. Chem. Int. Ed.* **2015**, *54*, 6521–6525; *Angew. Chem.* **2015**, *127*, 6621–6625.
[39] T. Grancha, A. Acosta, J. Cano, J. Ferrando-Soria, B. Seoane, J. Gascon, J. Pasán, D. Armentano, E. Pardo, *Inorg. Chem.* **2015**, *54*, 10834–10840.
[40] M. Mon, A. Pascual-Álvarez, T. Grancha, J. Cano, J. Ferrando-Soria, F. Lloret, J. Gascon, J. Pasán, D. Armentano, E. Pardo, *Chem. Eur. J.* **2016**, *22*, 539–545.
[41] D. L. Rabenstein, *Acc. Chem. Res.* **1978**, *11*, 100–107.
[42] E. Pardo et al., *Angew. Chem. Int. Ed.* **2008**, *47*, 4211–4216; *Angew. Chem.* **2008**, *120*, 4279–4284.
[43] J. Rabone et al., *Science* **2010**, *329*, 1053–1057.
[44] C. Martí-Gastaldo et al., *Nat. Chem.* **2014**, *6*, 343–351.
[45] A. P. Katsoulidis et al., *Angew. Chem. Int. Ed.* **2014**, *53*, 193–198; *Angew. Chem.* **2014**, *126*, 197–202.
[46] J. E. Warren et al., *Angew. Chem. Int. Ed.* **2014**, *53*, 4592–4596; *Angew. Chem.* **2014**, *126*, 4680–4684.
[47] J. Vallejo, F. R. Fortea-Pérez, E. Pardo, S. Benmansour, I. Castro, J. Krzystek, D. Armentano, J. Cano, *Chem. Sci.* **2016**, *7*, 2286–2293.
[48] E. M. Nolan, S. J. Lippard, *J. Am. Chem. Soc.* **2007**, *129*, 5910–5918.
[49] T. Aridomi, K. Takamura, A. Igashira-Kamiyama, T. Kawamoto, T. Konno, *Chem. Eur. J.* **2008**, *14*, 7752–7755.
[50] S. Park, S. Y. Lee, S. S. Lee, *Inorg. Chem.* **2010**, *49*, 1238–1244.
[51] L. H. Gade, B. F. G. Johnson, J. Lewis, G. Conole, M. McPartlin, *J. Chem. Soc. Dalton Trans.* **1992**, *192*, 3249–3254.

[52] Preliminary results indicate that this selective recovery occurs even in the presence of other heavy metals such as Cd^{2+} and Pb^{2+}.
[53] D. Bradshaw, A. Garai, J. Huo, *Chem. Soc. Rev.* **2012**, *41*, 2344 – 2381.
[54] X. Feng, G. E. Fryxell, L.-Q. Wang, A. Y. Kim, J. Liu, K. M. Kemner, *Science* **1997**, *276*, 923 – 926.
[55] S. Bag, P. N. Trikalitis, P. J. Chupas, G. S. Armatas, M. G. Kanatzidis, *Science* **2007**, *317*, 490 – 493.

Received: June 21, 2016
Revised: July 26, 2016
Published online: August 16, 2016

